IEEE 802.11ax: Performance of OFDM Uplink Multi-User MIMO over Non-Ideal Scenarios

***Abstract*—We first present the motivations, challenges and issues that have been driven intensive research and design activities toward the specification of IEEE 802.11ax amendment, the sixth generation of wireless local networks (WLANs). Next, we summarize the main medium access control (MAC) protocols and physical layer (PHY) techniques that have been researched and developed in the scope of the IEEE Task Group (TG) 802.11ax. In the following, we derive a mathematical model for both uplink multi-user multiple input multiple output (UL MU-MIMO) transmission scheme and mean squared error (MMSE) MU-MIMO detector. After presenting a first order validation of an IEEE 802.11ax simulator, we show preliminary results on the performance of IEEE 802.11ax UL MU-MIMO transceivers. We conclude that reserving degrees of freedom at receiver side to allow diversity gains can mitigate the negative effects of imperfect channel state information (CSI), providing expressive power gains. We also have concluded that it is necessary to implement sophisticated channel estimation schemes and advance MIMO detectors to cope with the interference generated in uplink channels loaded with a large number of clients.**

Keywords*—WLANs; 802.11ax; 802.11ac; Uplink Multi-User MIMO; OFDM; MMSE, Channel Estimation.

I. INTRODUCTION

The first IEEE 802.11 wireless local area network (WLAN) standard was introduced in 1997 to operate in the 2.4 GHz industrial, scientific, and medical (ISM) band and specifies a maximum physical layer (PHY) data rate of 2 Mbps using either frequency hopping (FH) [1, pp.241] or direct-sequence (DS) [1, pp.253] spread spectrum modulation techniques. In 2016, almost two decades later, the main IEEE 802.11 medium access control (MAC) and PHY amendments to the original IEEE 802.11 spec are the IEEE 802.11n (2009, 540 Mbps), IEEE 802.11ac (2013, 7 Gbps), IEEE 802.11ah (Draft 7.0 2016, > 100 kbps) and IEEE 802.11af (2014, 568.9 Mbps).

IEEE 802.11nWLANs [2] can be deployed at both 2.4 GHz ISM and 5 GHz Unlicensed National Information Infrastructure (U-NII) bands. This amendment specifies a maximum PHY data rate of 260 Mbps and 540 Mbps [3] for bandwidths (BW) of 20 MHz and 40 MHz, respectively, when orthogonal frequency division multiplexing (OFDM) multiple input multiple output (MIMO) spatial division multiplexing (SDM) transmission scheme with four layers is implemented.

Fifth generation of WLANs (IEEE 802.11ac amendment [4]) can only operate in the 5 GHz U-NIII band using BW of 20/40/80/160/80+80 MHz; OFDM MIMO with up to eight spatial streams (SS); 2/4/16/64/256 quadrature amplitude modulation (M-QAM). The maximum PHY throughput is increased from 540 Mbps (802.11n, 40 MHz, 4x4 MIMO, 64-QAM) to almost 7 Gbps (802.11ac, 160 MHz, 8x8 MIMO, 256-QAM). The optional implementation of downlink (DL) multi-user (MU) MIMO techniques allows improving the network throughput when the system is loaded with stations (STAs) that have a lesser number of antennas than the number of antennas deployed at the access points (AP) due to the real world form factor and cost constraints [5].

IEEE 802.11ah amendment [6] targets low data rate and longer range applications in sub-GHz unlicensed bands for low power and low cost devices used in Internet of Things (IoT).

IEEE 802.11afamendment [7] (or Super Wi-Fi) defines spectrum sharing operation in TV white space spectrum (TVWS) in very high frequency (VHF) and ultra-high frequency (UHF) bands between 54 and 790 MHz. The main objective of IEEE 802.11af networks is to increase the coverage in sub-urban and rural areas since the shared use of sub-GHz spectrum allows increasing the coverage due to the excellent propagation characteristics in VHF and low UHF bands.

The Wi-Fi rollouts by telecom operators, the explosive traffic forecasted in ultra-dense networks, the demands of consumer and corporative market segments to increase the throughput with quality-of-service (QoS) have increased exponentially the Wi-Fi devices shipments (e.g., according with ABI Research 3B Wi-Fi chipsets were shipped globally in 2015 within a worldwide installed base of 5.3B Wi-Fi devices). Therefore, there are extraordinary business opportunities in the Wi-Fi market chain. On the other hand, the main drawbacks of current WLANs to achieve these market demands are: *(i)* the clear channel assignment (CCA) scheme is overmuch conservative reducing the network throughput in dense networks due to the frequent backoff of Wi-Fi radios; *(ii)* the MAC sequential channel access algorithm uses significant air time when there are STAs contending for resources to transfer heavy traffic, such as video and images; *(iii)* no narrowband is supported to multiplex low data rate devices used in IoT; *(iv)* the mechanisms implemented to protect legacy devices reduce the network efficiency.

The High Efficiency WLANs (HEW) Study Group (SG) was created in May 2013 with the following main targets: improve the *spectrum efficiency and area throughput* of 5-10 times in ultra-dense networks (notice that the IEEE 802.11ac amendment aimed at improving the *link throughput*); increase the real world performance in both indoor and outdoor deployments; boost power efficiency; operate within 2.4 GHz ISM and 5 GHz U-NII bands. The work developed at HEW SG led to the creation of Task Group (TG) 802.11ax in May 2014. A proposition for the Draft 1.0 was presented in March 2016 [8] and the publication of the Final IEEE 802.11ax Spec is forecasted to March 2019.

The remaining of this paper is organized as follows: Section II presents related works and our main contributions. Section III focuses on the design of uplink (UL) MU-MIMO

Roger Pierre Fabris Hoefel, Department of Electrical Engineering, Federal University of Rio Grande do Sul (UFRGS), Porto Alegre, Rio Grande do Sul (RS), Brazil; E-mail: roger.hoefel@ufrgs.br.

transceivers. Section IV investigates the performance of UL MU-MIMO transceivers over realistic WLANs scenarios, considering both system and hardware impairments. Finally, Section V draws our main conclusions and final remarks.

II. Related Works and Main Contributions

The IEEE 802.11ax main new PHY features are [8]: *(i)* DL and UL orthogonal OFDMA (users can be assigned to 2 MHz, 4 MHz and 8 MHz in addition to 20 MHz, 40 MHz, 80 MHz and 160 MHz to allow overhead reduction in the transmission of small packets and to provide OFDM gain from power pooling for users far from the access point); *(ii)* UL MU-MIMO (a symmetric counterpart to DL MU-MIMO specified in the IEEE 802.11ac amendment, as shown in Fig. 1); *(iii)* longer OFDM symbol (from 3.2 µs to 12.8 µs to obtain reliable operation on both indoor and outdoor environments). Notice that implementation of OFDMA and MU-MIMO enables three dimensional scheduling, i.e., time, frequency and space. Finally, we emphasize that the IEEE 802.11ax does not increase the BW and number of spatial streams beyond 160 MHz and 8, respectively, as specified in the IEEE 802.11ac amendment.

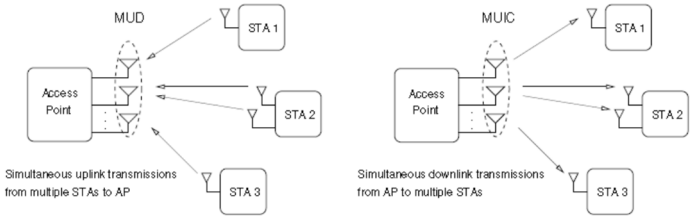

Figure 1. The left-side shows an example of UL MU-MIMO where three STAs are transmitting simultaneously to the AP in the same frequency block. A counterpart DL MU-MIMO is shown on the right-side [9].

The IEEE 802.11ax main MAC novel features are [8]: *(i)* new Carrier Sense Multiple Access (CSMA) protocol rules to implement CCA threshold level modifications that allow a more aggressive concurrent transmission in nearby cells within ultra-dense scenarios; *(ii)* control signaling for efficient resource utilization using new control fields that allow the STAs feed back their buffer status to optimize the UL schedule; *(iii)* efficient power mechanism using the Target Wake Time (TWT) inherited from IEEE 802.11ah amendment; *(iv)* MU protocol for UL/DL MU-MIMO/OFDMA.

Fig. 2 shows a UL MU-MIMO MAC protocol where the AP accesses the channel using the IEEE 802.11 random access Enhanced Distributed Coordination Function (EDCA) protocol [1]; obtains a transmit opportunity (TXOP); and sends a Trigger Frame (TF) to the STAs. The scheduled STAs respond after a predetermined time xIFS (Interframe Spacing) according with the mode defined by the TF, i.e., UL MU-MIMO in this particular example. The AP transmits a block acknowledgment (BA) frame using the DL MU-MIMO transmission mode. The TF contains both common information for all the STAs (e.g., duration of response, cyclic prefix length, etc.) and information specific per STA (resource allocation, modulation and code scheme, frequency and time synchronization, etc.).

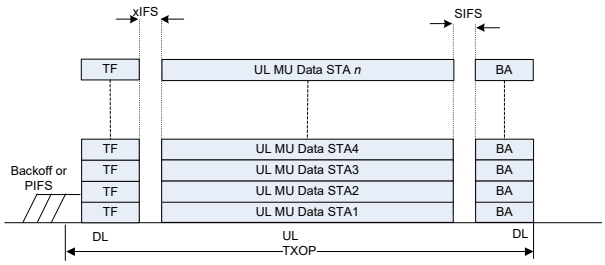

Figure 2 [8, pp. 32]."An example of a TXOP containing an UL MU transmission with an DL MU transmission containing unicast BA frames acknowledging the frames received from the respective STAs". SIFS means Short IFS.

In the framework of IEEE 802.11, the specification of UL MU-MIMO was proposed by Qualcomm researchers in 2009 during the standardization process of IEEE 802.11ac, driven by the "proliferation of UL data/video traffic from small-form factor devices that can support 1-2 spatial streams" [10]. However, the UL MU-MIMO was not included in the IEEE 802.11ac amendment [4]. Some technical challenges at PHY to implement UL MU-MIMO include: *(i)* samples of the cyclic prefix (CP) of the OFDM symbol must be used to mitigate the increase of inter-carrier interference due to timing errors, reducing, therefore, the number of CP samples used to mitigate the multipath in OFDM PHY; *(ii)* STAs may need to correct uplink transmissions for the frequency offset relative to the AP; *(iii)* clients may need to implement a power control scheme due to different path loss and shadowing among the STAs.

The implementation of UL MU transmissions schemes gained momentum with the creation of HEW SG. For instance, in [11] was carried out a comparative qualitative study on advantages, challenges and issues of the following MU techniques: OFDMA, MU-MIMO and code division multiplexing (CDM).

The benefits of control frequency and timing synchronization errors in OFDM system (e.g., the improved system performance and increased multipath tolerance) are still more important when UL MU techniques are implemented. Therefore, the TG 802.11ax [12] is considering to align their synchronization specifications (e.g., the IEEE 802.11ac specifies a transmit center frequency and symbol clock frequency tolerance of ±20 ppm for 5 GHZ band) with 3GPP requirements (e.g., Enhanced Node B frequency tolerance of ±0.05 ppm and ±0.1 ppm for wide area and local area environments, respectively).

The vast majority of the open literature on IEEE 802.11ax has been produced in TGax meetings by the major players of the wireless industry. The reference [13] is a peer-review tutorial that summarizes the motivations, challenges and issues related to research and design (R&D) activities toward the specification of 6G WLANs, i.e., the IEEE 802.1ax amendment.

The *main contribution* of this paper is to present an academically independent study, validated by first order analyzes, on the performance of UL MU-MIMO transceivers in the context of IEEE 802.11ax-based networks considering realistic aspects, such as, spatial and frequency-selective channel models, imperfect CSI, and frequency offset.

III. UPLINK MU-MIMO: TRANSCEIVER DESIGN

In OFDM MIMO PHY the signal processing operations are performed per subcarrier. In this paper, to avoid an overwhelming notation, we omit the superscript that specifies the subcarrier being processed when this can be perfectly understood from the context.

A. RECEIVED SIGNAL MODEL FOR UL MU-MIMO CHANNEL

The received symbols at the AP for an UL MU-MIMO OFDM channel loaded with *K* users can be modeled as

$$\boldsymbol{y} = \boldsymbol{H_{UL}}\boldsymbol{x} + \boldsymbol{z} = [\boldsymbol{H_1}, \boldsymbol{H_2}, \cdots, \boldsymbol{H_K}] \cdot \left[x_1, x_2, \cdots, x_{n_{t,total}}\right]^{\boldsymbol{T}} + \boldsymbol{z}, \quad (1)$$

where the UL MU-MIMO channel is given by the matrix $\mathbf{H_{UL}}$ with size n_r by $n_{t,total} = \sum_{u=1}^{K} n_{t,u}$; n_r is the number of receive antennas at the AP, and $n_{t,u}$ is the number of transmit antennas of the *u*th STA. The matrix $\mathbf{H_u}$, with size n_r by $n_{t,u}$, models the UL MIMO channel matrix observed at the AP due to transmission performed by the *u*th user.

The column vector $\mathbf{z}$ with size n_r models the zero mean circular symmetric complex Gaussian (ZMCSCG) noise. This vector is composed of n_r independent and identically distributed (i.i.d.) ZMCSCG random variables (r.v.) with variance N_0.

The vector of symbols at the output of the transmit antenna elements of the *u*th STA is given by $\boldsymbol{x_u} = \boldsymbol{P_u} \cdot \boldsymbol{s_u}$,where the symbols transmitted by the *u*th STA are modeled by the column vector $\boldsymbol{s_u} = \left[s_{u,1}, s_{u,2}, \cdots, s_{u,n_{ss,u}}\right]^{\boldsymbol{T}}$. The symbol transmitted by the *u*th STA at *j*th SS is denoted by $s_{u,j}$.

In the Draft 1 of IEEE 802.11ax [8] there is no support to transmit channel state information (CSI) from the AP to the STAs since in the UL MU-MIMO there is no need to implement beamforming at the transmitter side. However, the STAs must implement a fixed precoding scheme when it is necessary to match the number of SS with the number of antennas ports. For instance, a precoding matrix $\mathbf{P_u}$ used to map 2 SS to 4 transmit antennas at *u*th STA is given by (2), where the multiplicative constant is used to normalize the power. Notice that the matrix $\mathbf{P_u}$ has size $n_{t,u}$ by $n_{ss,u}$,where $n_{ss,u}$ denotes the number of SS transmitted by the *u*th STA.

$$\mathbf{P_u} = \sqrt{\frac{1}{2}} \cdot \begin{bmatrix} 1 & 0 \\ 0 & 1 \\ 1 & 0 \\ 0 & 1 \end{bmatrix}, \quad (2)$$

B. MMSE MU-MIMO DETECTORS

The received signal at the output of the MIMO detector due to the transmission of the *u*th STA can be modeled by the column vector $\boldsymbol{y_u}$ with size $n_{ss,u}$ as follows:

$$\boldsymbol{y_u} = \boldsymbol{W_u^H}\boldsymbol{y_u} = \boldsymbol{W_u^H} \cdot (\boldsymbol{H_{UL}}\boldsymbol{x} + \boldsymbol{z}), \quad (3)$$

where the matrix $\mathbf{W_u}$, with size n_r by $n_{ss,u}$, denotes the linear MIMO detector for the *u*th STA.

Denoting the effective channel matrix observed by the MIMO detector of *u*th user at the AP as $\boldsymbol{H_u}$, with size n_r by $n_{t,u}$, then the UL MU-MIMO channel matrix can be rewritten as

$$\boldsymbol{H_{UL}} = [\boldsymbol{H_1}, \cdots \boldsymbol{H_u}, \cdots, \boldsymbol{H_K}], \quad (4)$$

where $\boldsymbol{H_u}$ has size n_r by $n_{t,u}$. The columns of $\boldsymbol{H_u}$ contains the columns of $\boldsymbol{H_{UL}}$ that correspond to the UL MIMO channel between the *u*th STA and the AP.

Incorporating the effects of precoding, then (4) can be rewritten as

$$\widetilde{\boldsymbol{H}}_{\boldsymbol{UL}} = \left[\widetilde{\boldsymbol{H}}_{\boldsymbol{1}}, \cdots, \widetilde{\boldsymbol{H}}_{\boldsymbol{u}}, \cdots, \widetilde{\boldsymbol{H}}_{\boldsymbol{K}}\right] = [\boldsymbol{H_1}\boldsymbol{P_1}, \cdots, \boldsymbol{H_u}\boldsymbol{P_u}, \cdots, \boldsymbol{H_K}\boldsymbol{P_K}], \quad (5)$$

where $\widetilde{\boldsymbol{H}}_{\boldsymbol{u}}$ has size n_r by $n_{ss,u}$.

Using (5), the output of the MIMO detector for the *u*th STA can be rewritten as

$$\boldsymbol{y_u} = \boldsymbol{W_u^H} \cdot \left(\left[\widetilde{\boldsymbol{H}}_{\boldsymbol{1}}, \cdots, \widetilde{\boldsymbol{H}}_{\boldsymbol{u}}, \cdots, \widetilde{\boldsymbol{H}}_{\boldsymbol{K}}\right]\boldsymbol{s} + \boldsymbol{z}\right), \quad (6)$$

where the symbols transmitted by all *K* STAs are modeled by the column vector $\mathbf{s} = \left[\mathbf{s_1^T}, \mathbf{s_2^T}, \cdots, \mathbf{s_K^T}\right]^{\mathbf{T}}$ with size $n_{ss,total}$, where $n_{ss,total} = \sum_{u=1}^{K} n_{ss,u}$.

Therefore, using (6), the MMSE MU-MIMO detector for the *u*th user is given by

$$\boldsymbol{W_{MMSE,u}} = \left[\widetilde{\boldsymbol{H}}_{\boldsymbol{UL}}(\widetilde{\boldsymbol{H}}_{\boldsymbol{UL}})^{\boldsymbol{H}} + \frac{\boldsymbol{I_{n_r}}}{\boldsymbol{SNR_u}}\right]^{-\boldsymbol{1}} \widetilde{\boldsymbol{H}}_{\boldsymbol{u}}, \quad (7)$$

where SNR_u denotes the signal-to-noise ratio (SNR) observed at the MIMO detector input for the *u*th STA.

Eq. (7) shows that the very-high throughput long training (VHT-LTF) fields must have a number of SSs specified by (8), i.e., the SSs transmitted to all users must be considered in order to estimate the matrix $\widetilde{\boldsymbol{H}}_{\boldsymbol{UL}}$with size n_r by $n_{ss,total}$ [14-15].

$$N_{LTF} = \begin{cases} n_{ss,total} & if\ n_{ss,total} = 1, 2, 4, 6, 8 \\ n_{ss,total} + 1 & if\ \ n_{ss,total} = 3, 5, 7 \end{cases}. \quad (8)$$

IV. PERFORMANCE ANALYZES

Tab. I shows the main characteristics of the IEEE 802.11ac/ax simulator that we have been working on [8, 17]. In this paper, we assume a BW of 80 MHz and soft-decision Viterbi decoding.

In this section, we analyze the performance of UL MU-MIMO 802.11ax PHY for modulation and code schemes (MCS) shown in Tab. II. Notice that 6 STAs, transmitting simultaneously 1 SS each using MCS3, produces a total PHY rate of 702 Mbps.

Table I– Parameters of IEEE 802.11ac/ax simulator [8,17].

Parameter	Value	Parameter	Value
Carrier Frequency	5.25 GHz	**MCS**	0-9
Bandwidth	20 MHz, 40 MHz, 80 MHz	**Number of Spatial Streams**	1 to 8
GI Length	800 ns	**Synchronization**	Auto-Correlation
Modulation	BPSK, QPSK, 16-QAM, 64QAM, 256-QAM	**MIMO Channel Estimation [21]**	Least Squares
Binary Convolutional Code (BCC)	Code rate: r=1/2, r=2/3, r=3/4, r=5/6	**Channel Decoder**	Hard and Soft-Decision Viterbi Decoding

Table II - MCS investigated in this paper. The PHY data rates assume a guard-interval (GI) of 800 ns and BW of 80 MHz.

MCS	Mod	BCC Code Rate	# SSs	Data Rate Mbps
0	BPSK	1/2	1	29.3
3	16-QAM	1/2	1	117.0

Hereafter, a UL MU-MIMO channel labeled as $[n_t,n_r,K,n_{ss}]$ have the following characteristics: *(i)* each STA has an equal number of n_t transmit antennas; *(ii)* the AP has n_r receive antennas; *(iii)* the channel is loaded with *K* STAS; *(iv)* each STA transmits an equal number of n_{ss} SS.

The simulation results assume the spatial correlated and frequency selective TGac D channel model [14], which models a typical office channel with maximum excess delay of 390 ns and root mean square (rms) delay spread of 50 ns [3, pp. 38].

A. First Order Validation

A validation of the IEEE 802.11ac/ax simulator that we have been developing is presented in [17]. In this subsection, our simulation results for the MAC protocol data unit (MPDU) uncoded bit error rate (BER) at the Viterbi input (raw BER) assuming an UL MU-MIMO 802.11ax system are compared with analytical results [18, 19] and results from the open literature [20].

Fig. 3 shows the raw BER as function of the SNR per bit (E_b/N_0) over an i.i.d. flat fading Rayleigh MIMO channel (i.e. the canonical MIMO channel). The analytical results for QPSK [18] and 16-QAM [19] assume a single input single output (SISO) link. The simulation results from [20] consider a single-carrier SU MIMO system, where just one STA transmits 2 SS to an AP equipped with 2 antennas (i.e., a [2,2,1,2] MIMO channel). The simulation results from [20] postulate perfect synchronization and channel estimation. Therefore, in this figure our shown simulation results also assume perfect synchronization and channel estimation in order to have an unbiased comparison with [20]. Basically, we can verify a good agreement between the results from different sources. Notice that even using analytical results obtained for SISO systems, these outcomes follow closely the results for SU and MU-MIMO since the uncorrelated nature of the canonical MIMO channel minimizes the effects of intra-stream interference in MIMO channels with low spatial dimensionality. Finally, we emphasize that it is a complex task to establish comparisons based on a tight match among simulation results obtained from different sources due to the myriad of parameters and assumptions necessary to implement complex PHY layer simulators.

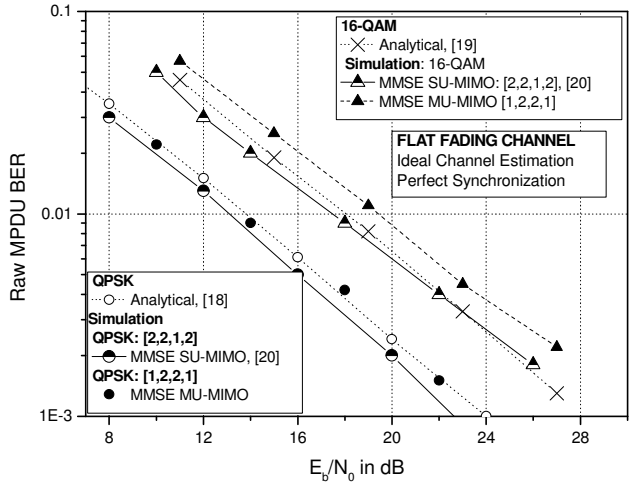

Figure 3. Raw MPDU BER a function of SNR per bit over canonical flat fading SISO and MIMO channels.

B. Effects of Imperfect CSI

Figures 4a (MCS0) and 4b (MCS3) shows the PER as function of SNR in dB for the following channel configurations: *(i)* Flat [1,2,2,1]; *(ii)* Flat [1,4,2,1]; *(iii)* TGac D [1,2,2,1]; *(iv)* TGac D [1,4,2,1]. These results are also parameterized by the type of channel estate information available at the MIMO receiver, i.e. LS [21] and perfect CSI. In this paper, we define perfect CSI when the noise is not taken into account in the LS channel estimation scheme.

Fig 4a shows that the use of spatial diversity at receiver side allows an expressive power gain since a SNR of 17 dB to obtain a PER of 1% is necessary for the canonical flat fading [1,4,2,1] channel, while a SNR of ~25 dB is demanded for the canonical flat fading [1,2,2,1] channel. The results depicted for the TGac D [1,4,2,1] channel show a large power loss when realistic LS channel estimation is implemented in the low power regime.

Fig 4b shows that the use of spatial degrees of freedom to provide diversity gain at receiver side allows more than 15 dB of power gain when the 16-QAM modulation scheme is used. These results also show, comparing the rate of PER vs. SNR, that the frequency selective TGac D channel has a great frequency diversity in relation to the canonical MIMO channel. Finally, notice that since the system operates at medium power regime when the MCS3 (16-QAM) is used, then the effects of neglecting the noise at CSI are not so relevant in relation to systems that operate in low power regime, as exemplified in Fig. 4a by the two leftmost curves, where the MCS0 (BPSK) is transmitted over the *TGac D [1,4,2,1]* canonical channel.

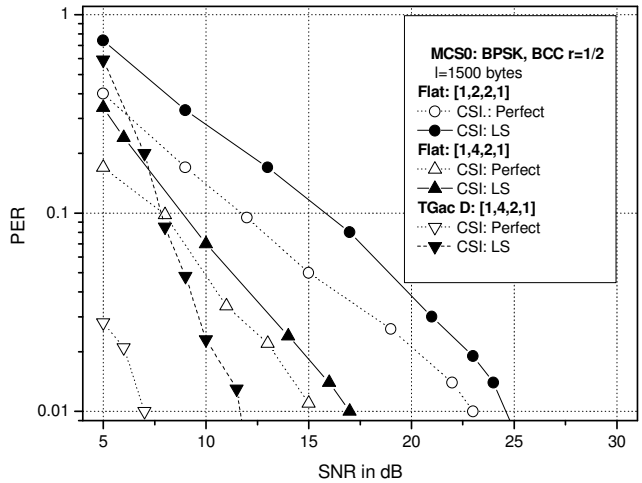

Figure 4a. MCS0: BPSK, BCC with code rate 1/2.

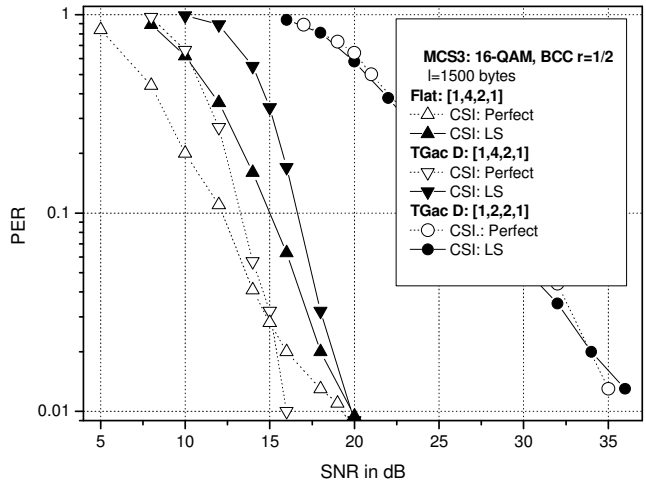

Figure 4b. MCS3: 16-QAM, BCC with code rate 1/2.

Figure 4. PER a function of SNR over canonical flat fading and TGac D MU-MIMO channels: effects of CSI (perfect or LS) on the system performance.

B. Effects of High Number of STAs and Frequency Offset

Fig. 5 shows the MPDU PER vs. the SNR in dB when the channel is loaded with six clients in order to study the effects of channel load on the UL MU-MIMO transceiver performance. Notice that in this set up a SNR of 27.5 dB and 39 dB are necessary to get a PER of 1% for MCS0 and MCS3, respectively, over the TGac D [1,8,6,1] channel. On the other hand, Fig. 4 shows that SNR of 17.5 dB and 23 dB are demanded for MCS0 and MCS3, respectively, over the canonical i.i.d. flat fading MU-MIMO channel.

This figure also shows results when an *equal absolute frequency offset i*s introduced for all clients. Analyzing these results, we can conclude that the frequency offset estimation and residual phase tracking algorithms described and analyzed in [22] is robust enough to mitigate the absolute common frequency offset in the IEEE 802.11ax UL MU-MIMO scenario.

The normalized frequency offset in OFDM PHY is defined as [23, pp.27]

$$\varepsilon = \frac{\Delta f}{\Delta_F}, \tag{9}$$

where Δf and ΔF denote the frequency offset and subcarriers spacing, respectively. The subcarriers spacing in the IEEE 802.11ax systems is *312.5 kHz* and the maximum frequency offset is ± 232 *kHz* (± 20 *ppm)*, resulting in $|\varepsilon| \cong 0.74$.

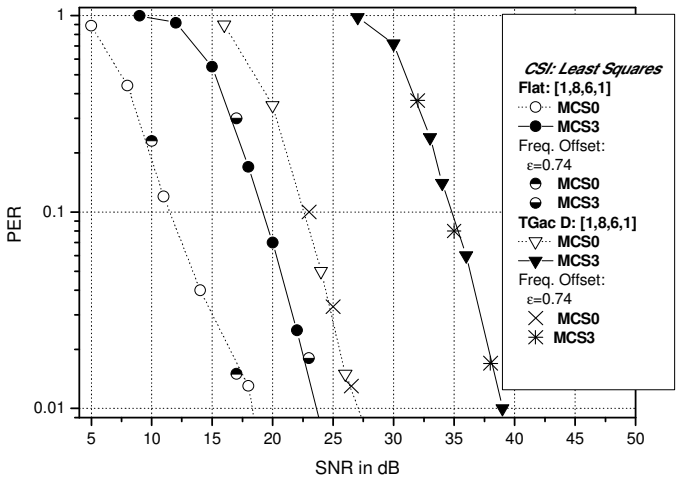

Figure 4. MPDU PER a function of SNR over canonical flat fading and TGac D MU-MIMO channels: effects of MCS and frequency offset on the system performance.

IV. CONCLUSIONS

First, we summarized the motivations, MAC and PHY challenges and issues that have driven the development of the IEEE 802.11ax amendment. Second, we developed a mathematical model for an IEEE 802.11ax UL MU-MIMO transceiver that implements MMSE MIMO detector. In the following, we presented preliminary simulation results of the MPDU PER as function of the SNR in dB, validated using a first order approach, for the performance of an IEEE 802.11ax UL MU-MIMO transceiver with MMSE MU-MIMO detector operating over flat fading canonical and spatial-correlated, frequency selective MIMO channels. We also analyzed the effects of absolute frequency offset on the system performance.

Finally, we have concluded that it is necessary to implement sophisticated channel estimation schemes and advance MIMO detectors to cope with the interference in uplink channels loaded with a large number of clients.

In our following R&D activities, we plan to design and optimize IEEE 802.11ax UL MU-MIMO transceivers that have robustness in relation to channel load, channel delay, different received power and relative frequency offset.

REFERENCES

[1] M. S. Gast, *802.11 Wireless Networks*. O'Reilly, 2005.

[2] Wireless LAN Medium Access Control (MAC) and Physical Layer (PHY) Specifications, Amendment 5: Enhancement for Higher Throughput, IEEE Std 802.11n-2009, 2009.

[3] E. Perahia and R. Stacey, *Next Generation Wireless LANS*: *802.11n and 802.11ac.2th ed*. Cambridge: Cambridge University Press, 2013.

[4] Wireless LAN Medium Access Control and Physical Layer Specifications, Amendment 5: Enhancement for Very High Throughput for Operations in Bands below 6 GHz. IEEE P802.11ac, Dec., 2013.

[5] O. Bejarano, R. P F. Hoefel, E. Knightly. "Resilient, multi-user beamforming WLANs: mobility, interference and imperfect CSI," *IEEE International Conference on Computer Communications (IEEE INFOCOM 2016)*, San Francisco, USA, 2016.

[6] VK Jones and H. Sampath. "Emerging technologies for WLAN," in *IEEE Communication Magazine,* vol. 53, no. 3, pp. 141-149, March, 2015.

[7] A. B. Flores et. al. "IEEE 802.11af: a standard for TV white space spectrum sharing," *IEEE Communications Magazine,* vol. 51, no. 10, pp. 92-100, Out., 2013.

[8] R. Stacey. *Proposed TGax draft specification.* IEEE 802.11-16/0024r1, March 2016.

[9] R. Liao, B. Bellalta, M. Oliver and Z. Niu. "MU MIMO MAC protocols for Wireless Area Networks: a survey,"arXiv:1404.1622, Nov. 2014

[10]R. V. Nee et. al.*UL MU-MIMO for 11ac*. IEEE 802.11-09/0852-00-00ac, July, 2009.

[11] J. Chun et. al.*Uplink multi-user transmission*. IEEE 11-13/1388r0, Nov., 2013.

[12] Y. Fanget. al.*MU synchronization requeriments for SFD.* IEEE 802.11-15/0363r1, March 2015.

[13] B. Bellalta. "IEEE 802.11ax: High-efficiency WLANS,".*IEEE Wireless Communications*, vol. 23, no. 1, 38-46, Jan. 2016.

[14] S. Veramani and A. V. Zelst. *Interference cancellation for downlink MU-MIMO*. IEEE 802.11-09/1234r1, 2010.

[15] R. P. F. Hoefel. "IEEE 802.11ac: on lessons learned on OFDM MU-MIMO transceivers with realistic feedback over TGac Channels with dopplerspread,"in *20th IEEE International ITG Workshop on Smart Antennas,* Munich, March 2016.

[16] G. Breit, H. Sampath, S. Vermani, et. al. *TGac Channel Model Addendum Support Material.* IEEE 802.11-09/06/0569r0, May, 2009.

[17] R. P. F. Hoefel. "Multi-User OFDM MIMO in IEEE 802.11ac WLAN: a simulation framework to analysis and synthesis", in *IEEE Latin America Transactions,* vol.13, no. 2, pp.540-545, Feb., 2015.

[18] J. G Proakis, "*Digital Communication - 5thed,"* New York: McGraw-Hill, 2007.

[19] L. Yang and L. Hanzo, "A recursive algorithm for the error probability evaluation of *M*-QAM," IEEE Communications Letters, vol. 4, n. 10, p. 304-306, October 2000.

[20] L. Bai and J. Choi, *Low Complexity MIMO Detection*. New York: Springer, 2012.

[21] R. P. F. Hoefel, "IEEE 802.11n: On the performance of channel estimation schemes over OFDM MIMO spatially-correlated frequency selective fading TGn channels," *XXX Brazilian Symposium on Telecommunications*, Brasília, Brazil, 2012.

[22] R. P. F. Hoefel. "On the synchronization of IEEE 802.11n devices over frequency selective TGn channel models," *25th Annual Canadian Conference on Electrical and Computer Engineering (CCECE 2012),* Montreal, 2012.

[23] R. Spitschka, *Synchronization Algorithms for OFDM Systems Using the Example of WLAN*. Saarbrucken, Germany: VDM Verlag, 2008.